Deep-Sea Research I 83 (2014) 115–123

Contents lists available at ScienceDirect

Deep-Sea Research I

journal homepage: www.elsevier.com/locate/dsri

Alkenones as tracers of surface ocean temperature and biological pump processes on the Northwest Atlantic margin

Jeomshik Hwang [a,b,*], Minkyoung Kim [a], JongJin Park [c], Steven J. Manganini [b], Daniel B. Montluçon [b,d], Timothy I. Eglinton [b,d]

[a] POSTECH (Pohang University of Science and Technology), Pohang 790-784, South Korea
[b] Woods Hole Oceanographic Institution, Woods Hole, MA 02543, USA
[c] Kyungpook National University, Sangju, South Korea
[d] ETH Zürich, 8092 Zürich, Switzerland

ARTICLE INFO

Article history:
Received 11 May 2013
Received in revised form
7 October 2013
Accepted 10 October 2013
Available online 25 October 2013

Keywords:
Alkenone temperature
Particulate organic matter
New England slope
Lateral transport
Alkenone unsaturation index

ABSTRACT

We have examined alkenone distributions, specifically the temperature proxy $U^{K'}_{37}$, in sinking particulate organic matter (POM) intercepted at three depths by time-series sediment traps deployed between 2004 and 2007 on the Northwest Atlantic margin. The goal was to assess physical and biogeochemical processes acting upon alkenones during passage through the water column. $U^{K'}_{37}$ did not exhibit any systematic trend with increasing depth despite several-fold attenuation in alkenone flux. Because of the extensive reduction in C_{37} alkenone flux in the water column and more efficient alkenone degradation during the period of high alkenone flux, the temperature bias toward that of more productive seasons was reduced with increasing trap depth. The temporal variation of $U^{K'}_{37}$ and alkenone-derived temperature compared best with the satellite-derived SST at an upstream region approximately 160 km east of the mooring site with a time lag of about 30 days, suggesting this region as the dominant source of alkenone-bearing POM. The alkenone-derived temperature of core-top sediments (15 °C) at the study site was lower than the flux-weighted average alkenone-derived temperature of sinking POM at 50 m above the seafloor. This discrepancy may reflect additional supply of resuspended sediment carrying alkenones produced in cooler waters to the northeast, and transported in bottom nepheloid layers.

1. Introduction

Since the first discovery of the relationship between alkenone unsaturation and the temperature of water where the organisms grow (Brassell et al., 1986; Prahl and Wakeham, 1987), the alkenone unsaturation index ($U^{K'}_{37}$) proxy, defined as a ratio of di-unsaturated C_{37} methyl ketone ($[C_{37:2}]$) to the sum of di- and tri-unsaturated C_{37} methyl ketones ($[C_{37:2}+C_{37:3}]$), has been widely used in paleoceanographic reconstructions (for example, Sachs et al., 2000; Herbert, 2003). One persistent question is why $U^{K'}_{37}$ of surface sediment is correlated strongly with mean annual sea surface temperature (SST) despite strong seasonal variations in alkenone production and export flux that could potentially bias the temperature towards periods of maximum growth. This temperature bias may thus be more severe over continental margins where rapid transit to sediment and high sedimentation rates may not provide enough time for remineralization of the pulse of sinking particulate organic matter (POM). However, this process has yet to be confirmed by field studies.

A related issue is whether $U^{K'}_{37}$ is altered by various biotic and abiotic degradation during passage through the water column and subsequent burial (see a recent review of Rontani et al., 2013 and references therein). Tiered sediment trap arrays are useful tools for answering these questions since they facilitate examination of how alkenones signals (e.g., $U^{K'}_{37}$ values) are transferred from surface waters to depth (for example, Rosell-Melé and Prahl, 2013).

In addition to the application of $U^{K'}_{37}$-derived temperature (hereafter $T_{alkenone}$) for reconstruction of past ocean conditions, alkenones can provide insights into the oceanic processes that influence POM cycling. In particular, because these compounds are exclusively synthesized by a specific class of marine phytoplankton, they serve as excellent tracers of alkenone-bearing POM derived from surface ocean productivity. One example is the use of these compounds to reveal an important role for lateral transport in the dispersal of POM by ocean currents, especially on the continental margins (Benthien and Müller, 2000; Mollenhauer et al., 2006; Ruhlemann and Butzin, 2006; Hwang et al., 2009a; Kusch et al., 2010). $U^{K'}_{37}$ measurements

* Corresponding author at: Ocean Science and Technology Institute, POSTECH (Pohang University of Science and Technology), Pohang 790-784, South Korea. Fax: +82 54 279 9519.
E-mail addresses: jhwang@postech.ac.kr, jeomshik@gmail.com (J. Hwang).

0967-0637/$ - see front matter © 2013 Elsevier Ltd. All rights reserved.
http://dx.doi.org/10.1016/j.dsr.2013.10.003

combined with radiocarbon analysis of alkenones have revealed long-range transport of organic matter associated with resuspended sediments (Ohkouchi et al., 2002). By comparison of temporal variations in $T_{alkenone}$ of sinking POM intercepted at depth with that of SST, insights on the processes such as packaging and export of POM, and sinking speed of particles may be gained (Knappertsbusch and Brummer, 1995; Müller and Fischer, 2001; Conte et al., 2003). Temperate oceans, with large seasonal variations in SST are especially appropriate for this application due to high-amplitude variations in $T_{alkenone}$ that can be tracked through the water column.

A recent time-series biogeochemical flux study was established to examine POM cycling on the NW Atlantic margin (Hwang et al., 2009a). This region of the New England slope has been the subject of a sustained physical oceanographic observation program designed to explore the variability of the Deep Western Boundary Current (DWBC), a deep limb of the Atlantic meridional overturning circulation, and the Gulf Stream system (Joyce et al., 2005; Toole et al., 2011). A particular focus of this time-series study was an assessment of the influence of the DWBC and associated lateral particle transport on the biogeochemical properties of sinking and suspended particles and bottom sediments along the path of this undercurrent (Hwang et al., 2009a, 2009b). Radiocarbon measurements in association with other biogeochemical data such as aluminum concentrations and long-chain saturated fatty acid concentrations indicated that supply of laterally transported resuspended sediment contributed considerably to sinking and suspended POM at the study site (Hwang et al., 2009a, 2009b). As a part of this time-series biogeochemical flux study, we utilize $U^{K'}_{37}$ data as a window into POM cycling over this highly productive continental margin. We also take advantage of the $U^{K'}_{37}$ data of sinking POM to provide insights into some of the unresolved questions mentioned above concerning the transfer of molecular proxy signals emanating from surface waters to depth.

2. Methods

Various types of samples were collected on the NW Atlantic margin from 2004 to 2007.

Three conical sediment traps (McLane Mark-7, Honjo and Doherty, 1988) were deployed at three nominal depths – 1000 m, 2000 m, and 3000 m (~50 m above the bottom) – on a single bottom-tethered mooring on the NW Atlantic margin (39°28′N, 68°22′W; Fig. 1; see Table 1 for details of trap depths, bottom depths, and sampling intervals for the three deployments). Sinking particles were collected from June 27, 2004 to April 27, 2005, from July 1, 2005 to June 1, 2006, and from June 27, 2006 to June 1, 2007. About 5 g/L of sodium chloride was added to seawater that was used to fill the collection cups. For 2004–5, and 2005–6 deployments, collection cups of the 1000 m and 2000 m traps were filled with seawater treated with various preservatives such as $HgCl_2$, formalin, Lugol's solution, DMSO (dimethyl sulfoxide), and HISTOCHOICE™ for the purpose of testing their relative efficiency for DNA preservation (Dennett and Manganini, 2006; not discussed further in this paper). Collection cups for the other samples were filled with seawater treated with $HgCl_2$ (0.3% by wt). Samples were stored at 4 °C until subsampling and further analyses. Each sieved sample (< 1 mm) was divided into ten equal aliquots using a wet sample splitter (WSD-10, McLane Research Laboratories, Inc.) and used for biogeochemical analyses.

Surface water suspended particles were collected by filtration of water from the ship's uncontaminated seawater intake (nominal sampling depth = 2.4 m) using 293 mm diameter filters (Gelman Science, type A/E glass fiber) for several hours per sample (Hwang et al., 2009b) during cruises aboard the R/V *Endeavor* in June 25–July 2, 2005 and the R/V *Oceanus* in June 22–27, 2006 (Table 2).

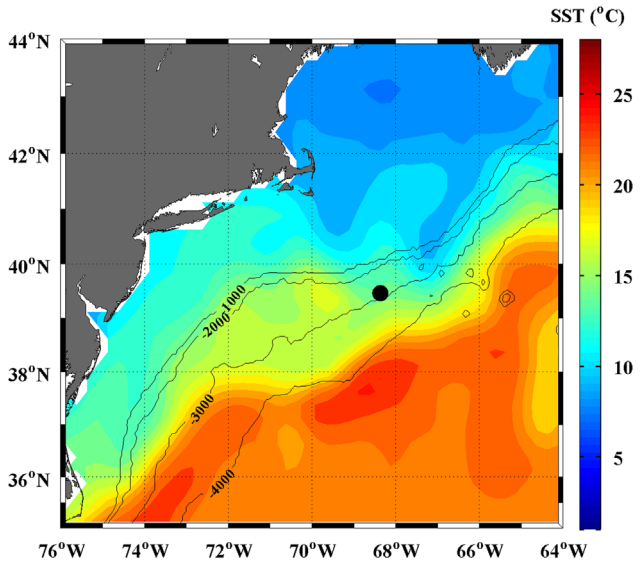

Fig. 1. Satellite-derived sea surface temperature (SST) on January 1, 2005 overlapped with bathymetry in the northwest Atlantic. Sediment trap mooring station is indicated.

Because the water was not pre-filtered using a large-mesh screen, the surface POM samples also include plankton. Each filter was folded and stored frozen at –20 °C in a pre-combusted aluminum foil pouch until analysis.

One tenth splits of each sediment trap sample, equivalent to ~30 to 4000 mg dry weight, were freeze-dried and used for determination of $U^{K'}_{37}$. Total lipid extracts were extracted into a mixture of methylene chloride and methanol (93:7 by volume) using an accelerated solvent extraction system (DIONEX ASE 200). Sample #9 of the 1000 m trap, 21 samples of the 2000 m trap, and samples #4, 6,8, 10, 12,14, 16, 18, 20 of the 3000 m trap from the 2006–7 deployment were extracted using a microwave accelerated reaction system (MARS, CEM Corporation) (these samples are indicated as half-filled symbols in Fig. 2). Although this has not been rigorously tested, we suspect that MARS has a greater extraction efficiency than ASE (Valier Galy, personal communication), as the saw-tooth concentration pattern observed for the 3000 m trap samples of the 2006–7 periods appears suspicious. However, this saw-tooth pattern was also observed for the 2000 m trap every sample of which was extracted using MARS. We have not found any suspicious pattern in $U^{K'}_{37}$ for the corresponding samples. This uncertainty does not affect our interpretation because the majority of the samples were extracted with the ASE system and hence the results maintain consistency. Also, our discussion on alkenone concentration and flux is focused on comparison among our own samples collected at different depths rather than comparison with other reported data.

Details of treatment of lipid samples for alkenone analysis have been published elsewhere (Hwang et al., 2009b). Alkenone concentrations and distributions were determined using an HP-5890II gas chromatograph/flame ionization detector (GC/FID) equipped with a capillary column (Varian, CP-SIL 5CB, 0.25 mm ID × 0.25 μm film thickness, either 60 m or 30 m in length) at Woods Hole Oceanographic Institution. 21 samples of the 2000 m trap from the 2006–7 deployment were analyzed using an Agilent 7890A GC/FID at ETH, Zürich. Alkenones were quantified by comparison to a C_{36} *n*-alkane external standard added immediately before injection to GC. Usually peaks of C_{37} alkenones are resolved well by baseline separation. However, for the samples #12 of the 1000 m trap and #19 of the 3000 m trap of 2006–7 deployment, the peaks of $C_{37:2}$ and $C_{37:3}$ were broad and incompletely separated resulting in erroneous peak area determination and consequently, no $U^{K'}_{37}$

Table 1
Sampling time, number of samples, time interval of each sample, trap depths, water depth for three deployments, and average values of alkenone – related properties.

	Sampling period (mm/dd/yy)	Water depth (m)	Trap depth (m)	Sampling interval (days)	# of samples	$C_{37:2}+C_{37:3,}$ average flux (μgC/m^{2}d) [min–max]	$C_{37:2}+C_{37:3,}$ average conc. (μg/g dry matter) [min–max]	$C_{37:2}+C_{37:3,}$ average conc. (mg/g POC) [min–max]	$U^{K'}_{37}$	Flux-weighted $U^{K'}_{37}$
1st year	06/27/04∼04/27/05	2988	968	23.38	13	3.9 [0.92–9.4]	24 [6.8–106]	0.26 [0.09–0.54]	0.675 [0.414–0.847]	0.732
			1976	14.48	21	1.3 [0.27–6.1]	7.3 [1.0–16]	0.13 [0.02–0.27]	0.694 [0.396–0.849]	0.623
			2938	14.48	21	1.0 [0.33–8.2]	4.1 [1.1–21]	0.08 [0.04–0.21]	0.665 [0.419–0.807]	0.557
2nd year	07/01/05∼06/01/06	2980	1011	25.77	13	3.7 [0.49–8.7]	25 [6.0–54]	0.28 [0.11–0.53]	0.688 [0.531–0.848]	0.736
			1968	15.95	21	1.1 [0.09–4.3]	6.1 [0.8–15]	0.10 [0.02–0.23]	0.731 [0.583–0.847]	0.734
			2930	15.95	21	0.65 [0.14–1.7]	3.5 [1.1–9.8]	0.08 [0.03–0.19]	0.681 [0.581–0.810]	0.693
3rd year	06/27/06∼06/01/07	2961	992	26.08	13	2.0 [0.18–3.7]	13 [4.6–22]	0.18 [0.05–0.28]	0.674 [0.487–0.862]	0.712
			1949	16.14	21	0.78 [0.12–2.5]	5.4 [0.8–21]	0.11 [0.02–0.39]	0.675 [0.386–0.859]	0.659
			2911	16.14	21	0.65 [0.09–3.3]	3.0 [0.4–9.9]	0.09 [0.02–0.25]	0.670 [0.417–0.832]	0.669
Entire period	06/27/04 ∼06/01/07		1000			3.2 [0.18–9.4]	21 [4.6–106]	0.24 [0.05–0.54]	0.679 [0.414–0.862]	0.730
			2000			1.1 [0.09–6.1]	6.3 [0.8–21]	0.11 [0.02–0.39]	0.699 [0.386–0.859]	0.670
			3000			0.78 [0.09–8.2]	3.5 [0.4–21]	0.09 [0.02–0.25]	0.672 [0.417–0.832]	0.621

Table 2
$T_{alkenone}$ of suspended POM samples collected from ship's clean seawater intake and the corresponding CTD temperature averaged over the surface mixed layer. The calibrations for surface water production and core-top sediment (values in parenthesis) by Conte et al. (2006) were used for $T_{alkenone}$.

Sample ID	Sample location and collection time	$U^{K'}_{37}$	$T_{alkenone}$ (°C)	CTD T (°C)	MLD (m)	ΔT[a]
EN407 Filter #7	39°28′N, 68°22′W Jun 27 2005, 02:26∼15:08	0.957[b]	27.4 (27.3)	26.5	12	+0.9 (+0.8)
EN407 Filter #12	38°37′N, 68°51′W Jun 29 2005, 02:34∼13:14	0.948[b]	27.1 (27.0)	27.6	33	−0.5 (−0.6)
EN407 Filter #21	39°45′N, 69°45′W Jul 1 2005, 10:22∼15:12	0.763[b]	22.3 (21.5)	22.8	46	−0.5 (−1.3)
OCE426 Filter #5	39°42′N, 69°07′W Jun 23 2006, 10:36∼18:34	0.738	21.7 (20.7)	21.2	40	+0.5 (−0.5)
OCE426 Filter #9	39°28′N, 68°16′W Jun 24 2006, 14:06∼20:30	0.737	21.7 (20.7)	24.0[c]	Not Defined	−2.3 (−3.3)
OCE426 Filter #12	38°33′N, 68°58′W Jun 26 2006, 07:33∼13:14	0.943	27.0 (26.8)	25.0	20	+2.0 (+1.8)
Average ± standard deviation						+0.0 ± 1.5 (−0.5 ± 1.8), +0.5 ± 1.0 (0.0 ± 1.3)[d]

[a] $\Delta T = T_{alkenone}$ − CTD T.
[b] These results have been reported by Hwang et al. (2009b).
[c] This value is an average temperature of the surface 20 m layer
[d] Average ± standard deviation when OCE426 filter #9 is excluded.

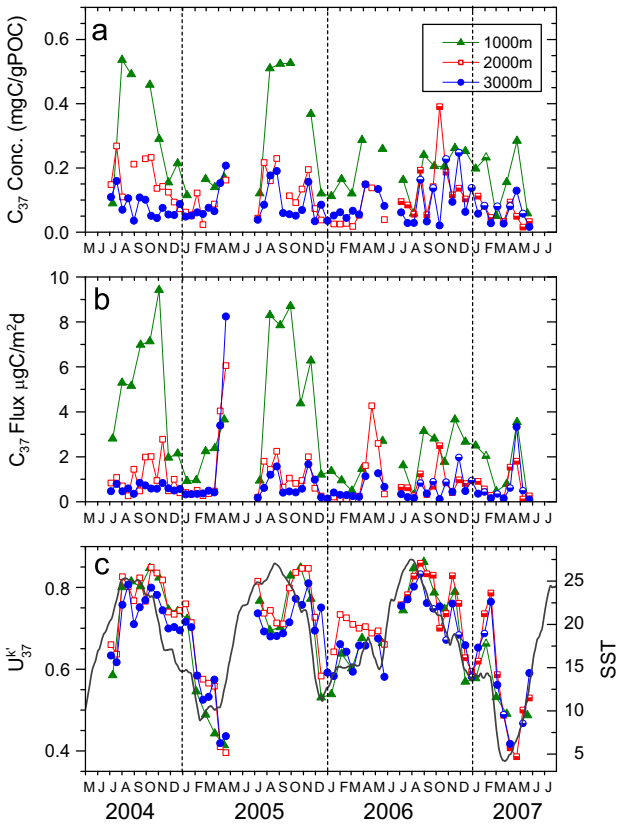

Fig. 2. Biogeochemical properties of sinking POM at 1000 m, 2000 m, and 3000 m nominal depths. (a) Concentration of di- and tri-unsaturated C_{37} alkenones normalized to POC, (b) flux of $C_{37:2}$ and $C_{37:3}$ alkenones in μgC/m^{2}d, and (c) temporal variation of $U^{K'}_{37}$ and satellite-derived SST (solid line) at the mooring site. Samples indicated as half-filled symbols were extracted with MARS (microwave accelerated reaction systems) instead of ASE (accelerated solvent extraction system).

results. The associated uncertainty and the standard deviation previously determined by analysis of core-top samples of 6 individual barrels from a single multi-core deployment at the trap mooring site was ±0.010 (average $U^{K'}_{37}$=0.559), corresponding to ±0.2 °C.

3. Results

3.1. Alkenone concentration and flux

C_{37} alkenone concentration in the 1000 m trap samples, represented as the sum of [$C_{37:2}$] and [$C_{37:3}$] normalized to POC concentration, ranged between 0.05 and 0.54 mgC/gPOC with a three-year average of 0.24 mgC/gPOC (Fig. 2a and Table 1). Alkenone concentrations at 1000 m depth exhibited considerable seasonal variability. The concentration was high in August, September, and October, especially in 2004 and 2005. The concentration was also elevated in late March and April in 2004 and 2005, although the magnitude was smaller compared to that in summer-early fall period. Concentrations also exhibited considerable interannual variability. During the 2006–7 period, the maximum concentration at 1000 m was not as conspicuous as in the other two deployment periods. C_{37} alkenone concentration decreased with sampling depth in general, by a greater extent between 1000 m to 2000 m than between 2000 m to 3000 m. The mean concentration was several-fold higher at 1000 m than at 2000 m and 3000 m (0.24 vs. 0.11 and 0.09 mgC/gPOC, respectively). The amplitude of temporal variability in concentration also decreased with increasing depth, with the peaks in the summer and early fall and in April becoming far less conspicuous.

C_{37} alkenone flux to the 1000 m trap ranged between 0.2 and 9.4 μgC/m^{2}d with a three-year average of 3.2 μgC/m^{2}d (Fig. 2b). In general, there was enhanced alkenone flux during August, September, and October, especially in 2004 and 2005. There was also another sharp increase in alkenone flux in April (Fig. 2b). These periods of high alkenone flux coincide with those of high alkenone concentration. Interannual variability in alkenone flux can be seen more clearly in Fig. 3. Year-to-year variability in alkenone flux appears to be large in August through October when maximum alkenone flux occurs (see Shutler et al., 2012 for timing of coccolithophore blooms in the North Atlantic). The enhanced flux in April appears more persistent. This time coincides with the spring bloom as reflected by maximum chlorophyll-a concentrations based on satellite observation (Yoder et al., 2001), although the spring bloom is mainly related to diatom productivity (Hwang et al., 2009a). The flux decreased substantially between 1000 m and 2000 m but by a much smaller amount between 2000 m and 3000 m. Variability in alkenone flux became smaller in concert with the marked reduction in alkenone flux.

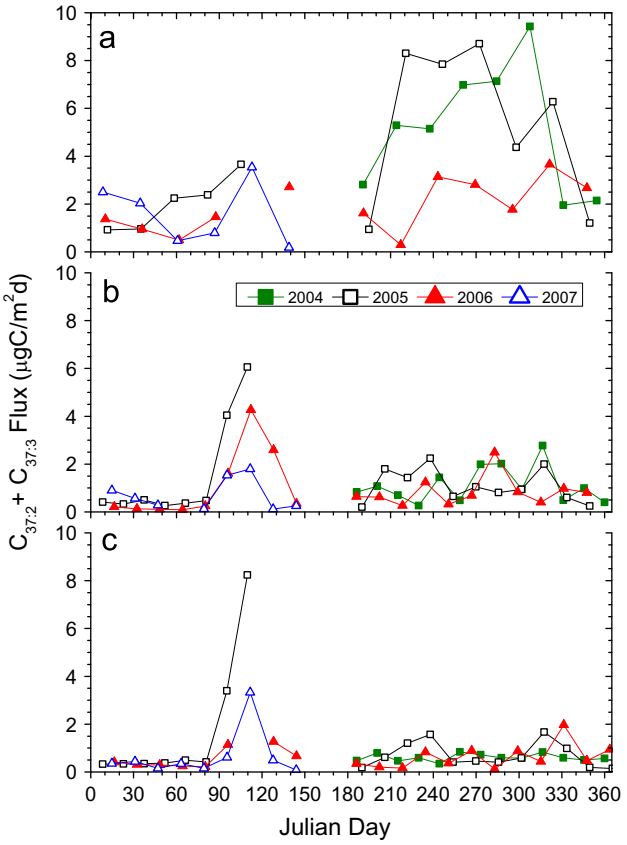

Fig. 3. Flux of $C_{37:2}$ and $C_{37:3}$ alkenones in each year at (a) 1000 m, (b) 2000 m, and (c) 3000 m.

3.2. Alkenone unsaturation index, $U^{K'}_{37}$

$U^{K'}_{37}$ values of sinking POM varied between 0.40 in April 2005 and 0.86 in early September in 2006 (Fig. 2c). A seasonal minimum in $U^{K'}_{37}$ was observed in April in 2005 and 2007. A noticeable anomaly was observed in the winter 2005–6, when $U^{K'}_{37}$ values were considerably higher than those in the other two years, and the seasonal minimum was observed in December and January. The seasonal variation in $U^{K'}_{37}$ values did not follow a smooth sinusoidal curve. Instead, abrupt increases and decreases were frequently observed. These deviations from a smooth curve, forming both dips and peaks, were often observed at more than one depth and thus considered a distinct natural phenomenon.

$U^{K'}_{37}$ values at the 3 depths temporally co-varied mostly within 0.1 (equivalent to about 3 degrees on the temperature scale), without showing any obvious time lag among the traps. The considerably higher $U^{K'}_{37}$ values at 2000 m than those at 1000 m and 3000 m in February and March, 2006 may be an exception. The three-year average $U^{K'}_{37}$ values were 0.679, 0.699, and 0.672 at 1000 m, 2000 m, and 3000 m depths, respectively, without showing any obvious trend with trap depth. In fact, the three-year average value at 2000 m was higher than those at 1000 m and 3000 m. Another interesting observation is that $U^{K'}_{37}$ values were higher (lower) at 1000 m than at 3000 m in the summer (winter) (see Fig. 7 also).

3.3. Comparison between $T_{alkenone}$ and SST

First, we examine whether alkenone-producing organisms reflect the seawater temperature faithfully at the study site by comparing CTD-measured temperature of the surface water with $T_{alkenone}$ of suspended POM collected by filtration of seawater from the ship's clean seawater intake for a few hours while the ship was at or in the vicinity of the sediment trap mooring site (Table 2). $T_{alkenone}$ estimated by both calibrations for global surface water production [$T_{alkenone}$ = −0.957 + 54.293 ($U^{K'}_{37}$) − 52.894 ($U^{K'}_{37}$)^2 + 28.321 ($U^{K'}_{37}$)^3] and core-top sediment [$T_{alkenone}$ = −1.334 + 29.876 ($U^{K'}_{37}$)] (Conte et al., 2006) mimicked CTD-measured temperature within the uncertainty of this temperature proxy (Table 2). Therefore, the $T_{alkenone}$ appear to reflect surface water temperature within a reasonable level of uncertainty at the study site, at least in the temperature range between 21.2 and 27.6 °C.

SST at the mooring site was not a smooth sinusoidal curve and fine-scale structure was evident, as in the temporal variation in $U^{K'}_{37}$ of sinking POM. When temporal variation in $U^{K'}_{37}$ was compared to that in SST at the mooring site, a time lag was apparent, especially between the maximal and minimal values of each property (Fig. 2c). The latter is somewhat expected considering the time lag between alkenone production and collection as sinking POM at depth. However, when $U^{K'}_{37}$ values were translated to temperature, $T_{alkenone}$ estimated by calibrations for global surface water production and core-top sediment ranged between ~14 °C and 24 °C, and between ~10 °C and 24 °C, respectively (also see web Supplementary Fig. S1). These temperature ranges were not identical to that of the SST at the mooring site (~5 °C to 27 °C). As suggested by Rosell-Melé and Prahl (2013), sinking POM may have different alkenone-related properties from suspended POM. We therefore used the calibration for core-top sediment (Conte et al., 2006) for temperature conversion for the subsequent discussion.

4. Discussion

4.1. Provenance of alkenone-bearing sinking POM

It is not feasible to establish the provenance of alkenone-bearing POM by examining the correlation between SST and $T_{alkenone}$, because seasonal fluctuations in SST would dominate the correlation between the two properties in the temperate ocean. However, short-term deviations from a smooth sinusoidal curve, which were apparent both in $U^{K'}_{37}$ and SST and reflect dynamic features such as the Gulf Stream and/or warm core rings, may provide clues on the source regions for alkenone-bearing sinking POM. The deviation in $T_{alkenone}$ was obtained by subtracting the $T_{alkenone}$ from a pure sinusoidal function fitting of the $T_{alkenone}$ time-series. For deviation in SST, the existing SST time-series data for the NW Atlantic (a daily product with 0.25° by 0.25° resolution provided by National Climatic Data Center, NOAA, which is optimally interpolated from AVHRR and AMSR satellite data; http://www.ncdc.noaa.gov/oa/climate/research/sst/griddata.php) were used. The daily SST data of each grid were bin-averaged in time for each sampling period of sinking POM. Then we determine the time lag between these two "de-seasoned" time-series data set that produces the best correlation.

The time lag appears to increase as the reference site moves away from the trap mooring site (Fig. 4a; only 3000 m trap results are shown; the results for all three traps are shown in web Supplementary Fig. S2). It shows that time lag values are positive toward the northeast, and negative toward the west. Because SST variation should lead $T_{alkenone}$ variation in time, the regions of negative time lags can be ignored. Fig. 4b shows the maximum correlation between the de-seasoned time-series of SST and $T_{alkenone}$ that are shifted by the corresponding time lag for each grid. The maximum correlation was found at around 66.5–67.5°W and 39.5–40°N, about 160 km east of the trap mooring site. For comparison of temperatures, root-mean-square values

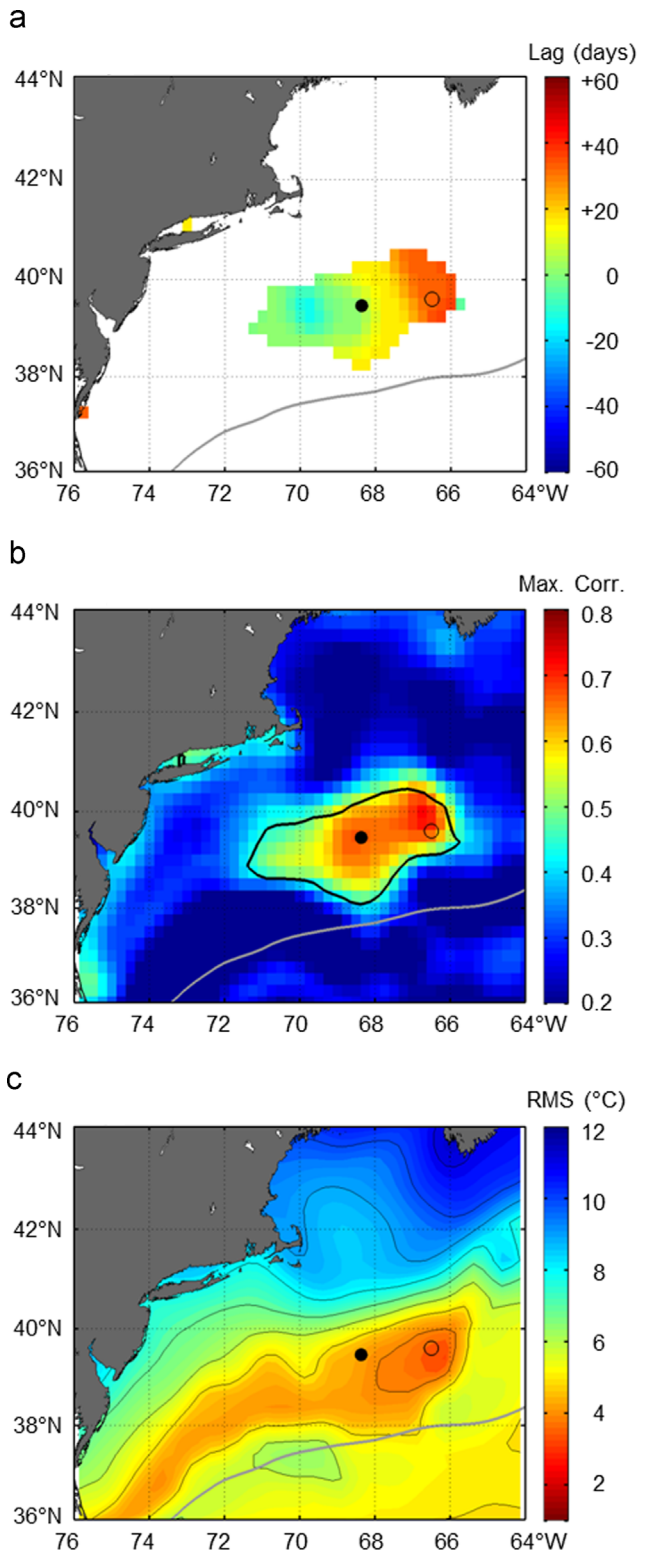

Fig. 4. Spatial distribution of (a) the time lag in days that maximizes the correlation presented in (b) between the de-seasoned SST and alkenone-derived temperature of 3000 m trap samples. Only data with > 99% statistical significance of the correlation are presented for the time lag. See text for the method of de-seasoning of the temperature data. (c) Root-Mean-Square in °C between alkenone-derived temperature of 3000 m trap samples and SST shifted by the corresponding time lag presented in (a). The black line in (b) denotes 99% of the statistical significance of the correlation. The gray line denotes the time-mean position of the Gulf Stream obtained from satellite altimeter data. The filled circle denotes the mooring station and the open circle denotes the site for which SST is presented in Fig. 5.

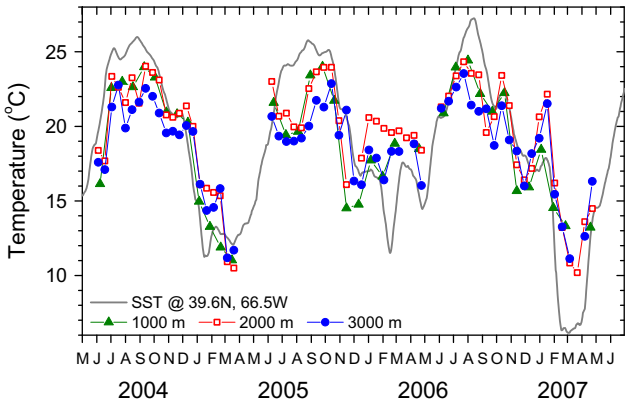

Fig. 5. Satellite-derived SST at 39.6°N and 66.5°W (solid line) and alkenone-derived temperatures shifted forward by 30 days.

($RMS \equiv \sqrt{(SST - T_{alkenone})^2/n}$, where n is the number of data) were calculated between SST and $T_{alkenone}$ that was shifted by the corresponding time lag. The lowest RMS values were obtained in the region slightly south of the region of maximum correlation (Fig. 4c). Together with the maximum correlation, the lowest RMS values at the location ~160 km east of the trap mooring site implies that the temporal variation in $T_{alkenone}$ of the sinking POC is most likely to be influenced by the SST upstream of the DWBC.

These results appear reasonable considering particle settling velocities up to a few hundred meters per day (Conte et al., 2001; Müller and Fischerm, 2001; Berelsonm, 2002) and a typical current velocity of 5 cm/s (4.3 km/day; Toole et al., 2011) of the prevailing DWBC current system. Sinking POM is expected to be transported southwestward to the site along the DWBC, once it settles below the upper layer of a few hundred meters that is sporadically influenced by warm core rings and the Gulf Stream. The $T_{alkenone}$ shifted forward by 30 days and SST at 39.6°N and 66.5°W are shown in Fig. 5 (and also Fig. S1) as an example. Considering the complex current system in the study region (Fig. 1), it is surprising that fine structure in temporal variations in $T_{alkenone}$ can be matched well with that of the SST.

The resultant distributions of time lag, maximum correlation, and RMS for the three trap depths were not different, perhaps with the exception that the time lags for 1000 m samples were slightly shorter than those for 2000 m and 3000 m samples (Fig. S2). This result implies that although there is time lag between production and initiation of sinking of POM, once initiated, sinking is fast enough to produce no distinction between the traps within the time frame of sampling resolution (2 weeks).

Considerable discrepancies do exist between $T_{alkenone}$ and SST values. As shown in Fig. 5, the best fit of $T_{alkenone}$ to the time-series data of SST results in lower $T_{alkenone}$ than SST during summer and higher $T_{alkenone}$ than SST during winter. Our results may imply that increasing the slope of the linear calibration equation will expand the predicted temperature range, and hence mimic the SST better (this issue was raised by F. Prahl upon reviewing the manuscript). However, more in-depth examination of the hydrographic data and modeling of the currents, potentially coupled with measurement of other geochemical tracers, will be necessary to pinpoint the actual "source funnels" of the collected sinking POM (Siegel and Deuser, 1997; Siegel et al., 2008) for more meaningful analysis of this type.

4.2. *Degradation of alkenones and its impact on* $U^{K'}_{37}$ *during the vertical transit*

In this section, we examine the potential alteration of $U^{K'}_{37}$ and flux-weighted $U^{K'}_{37}$ values in association with degradation of

alkenones during the vertical transit through the water column. From 1000 m to 3000 m, alkenone flux decreased on average by a factor of five. Also, alkenone concentration decreased by a factor of two. This may imply that alkenones are more prone to degradation compared to the bulk sinking POC. One possibility for the observed difference in alkenone concentration and flux at different sampling depths is that they reflect different source regions. However, the current field at the 3000 m isobath in this region is barotropically southwestward (Joyce et al., 2005; Toole et al., 2011). Because meridional SST gradient is large in this region, it is not very likely that sinking particles collected at 1000 m and 2000 m have originated from different locations that have similar SST but distinctly different E. hux productivity.

In the present study, $U^{K'}_{37}$ does not appear to show any clear systematic change with increasing sampling depth in the water column, despite the strong attenuation in the flux and concentration. We compared $T_{alkenone}$ after interpolation of the results of the 2000 m and 3000 m traps to fit the 23–26 day sampling intervals of the 1000 m trap (i.e., reducing the number of data points from 21 to 13 for each trap deployment). The average difference on a temperature scale corresponded to 0.7 °C (±1.3) and −0.1 °C (±1.8) between 2000 m and 1000 m, and between 3000 m and 1000 m, respectively (Figs. 2c and 7).

Although $U^{K'}_{37}$ values are not altered, flux-weighted $U^{K'}_{37}$ values can be altered by attenuation of alkenone flux. A few studies, including our own, which examined alkenone fluxes from tiered sediment traps have found that alkenone flux was attenuated much more extensively during the high alkenone-flux periods than low alkenone-flux periods (e.g., Harada et al., 2001; Müller and Fischer, 2001; Seki et al., 2007). If this is the case, temperature bias will be reduced and flux-weighted $T_{alkenone}$ may approach the annual average $T_{alkenone}$ or annual average SST. Indeed, alkenone flux at 3000 m exhibited much smaller seasonal variability than that at 1000 m (Fig. 2), presumably because of extensive degradation of alkenones. We compared C_{37} alkenone fluxes at 1000 m and 3000 m after interpolation of the flux values from the 3000 m trap to fit the 23–26 day sampling intervals of the 1000 m trap. The % reduction of C_{37} alkenone flux from 1000 m to 3000 m revealed a positive correlation with the C_{37} alkenone flux at 1000 m (Fig. 6). This finding demonstrates that degradation of alkenones occurs more efficiently during the high flux period. Consequently, flux-weighted $U^{K'}_{37}$ values decreased from 0.730 at 1000 m to 0.670 and 0.621 at 2000 m and 3000 m, respectively, showing that warm-temperature bias (in this specific case, warm-temperature bias is caused by elevated alkenone production mostly in summer) is reduced with increasing depth. Our results suggest that caution should be exercised when interpreting time-series data of $T_{alkenone}$ of sinking POM collected only at one depth, especially when the depth is not near the seafloor. Depending on particle interception depth, the flux-weighted $T_{alkenone}$ may not accurately reflect $T_{alkenone}$ that is ultimately transferred to the underlying sediments. The extent to which the temperature bias is reduced is likely to be influenced by parameters such as bottom depth (near shore vs. open ocean; Prahl et al., 1993), dissolved oxygen levels (Goni et al., 2001), exposure time to oxic degradation and so on. We postulate that, in the absence of other factors (e.g., see below), the temperature bias will be greater at near shore sites with short vertical transit times than at open ocean sites.

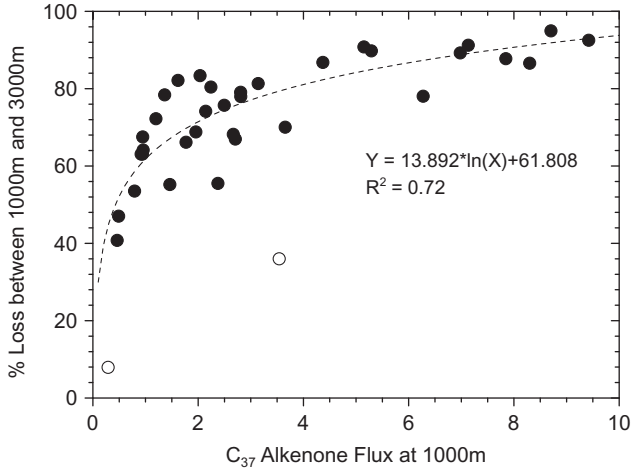

Fig. 6. Percent reduction in $C_{37:2}$ and $C_{37:3}$ alkenone flux from 1000 m to 3000 m relative to the flux at 1000 m. The regression equation was obtained excluding 4 data points (open circle), two of which were below zero because the flux at 3000 m was smaller than that at 1000 m (data not shown).

4.3. *Potential causes of* $U^{K'}_{37}$ *signal modification in sinking POM*

One interesting observation is that the $U^{K'}_{37}$ values at 3000 m were systematically lower than those at 1000 m in the summer, but were higher in the winter (Figs. 2 and 7). The difference was generally larger between 1000 m and 3000 m than between 1000 m and 2000 m. Diagenetic alteration would only result in an increase in $T_{alkenone}$ due to preferential degradation of the tri-unsaturated C_{37} ketone (Rontani et al., 2013 and references therein) and hence, is not likely the cause of the observed discrepancy.

One possible explanation is material exchange between sinking POM and suspended POM during the vertical transport in the water column. A $T_{alkenone}$ signal of suspended POM will represent the integral of production (and decomposition) over a longer time period (months to years Bacon et al., 1985), and hence, is expected to exhibit smaller seasonal variability than corresponding signals in sinking POM. The average $U^{K'}_{37}$ value of suspended POM observed in summer 2005 (0.654) was virtually constant from 1000 m to 2500 m, equivalent to 18.2 (±1.2) °C, much lower that the SST of the corresponding time (Hwang et al., 2009b). Therefore, inclusion of suspended POM to sinking POM in the water column would decrease the seasonal amplitude in $T_{alkenone}$ and hence may be responsible for the observed difference in $U^{K'}_{37}$ between depths. However, exchange between sinking POM and suspended POM is not well understood and a field of active research (Sheridan et al., 2002; Abramson et al., 2010).

Sinking POM likely also contains alkenones supplied from resuspended sediment whose $U^{K'}_{37}$ value is close to that of the annual average SST. Based on radiocarbon isotope mass balance, about 30% (±10%) of sinking POM collected in the three sediment traps during the 2004–5 period was estimated to be derived from lateral transport of resuspended sediment (Hwang et al., 2009a). The contribution of alkenones from sediment resuspension is, however, likely much smaller because of the difference in

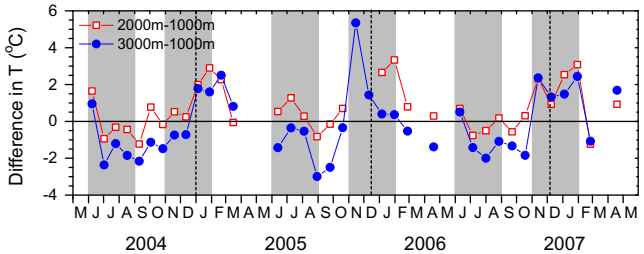

Fig. 7. Differences of alkenone-derived temperature between 1000 m and each 2000 m and 3000 m trap samples. Shaded bars denote June–August and November–January as representing summer and winter, respectively.

alkenone concentration between sinking POM and resuspended sediment.

4.4. Lateral supply of alkenones from resuspended sediment in the bottom nepheloid layer

The flux-weighted $U^{K'}_{37}$ value at 3000 m (0.621) is much closer to the $U^{K'}_{37}$ value of core-top sediment (0.559) at the trap mooring site than the corresponding value at 1000 m (0.730). Nevertheless, the $U^{K'}_{37}$ values correspond to a discrepancy of 1.8 °C between sinking POM at 3000 m and core-top sediment, with the latter recording a lower $T_{alkenone}$. While this discrepancy approaches the overall uncertainty inherent in this approach that stem from global calibrations, it is well beyond analytical uncertainty and one would anticipate closer agreement between water column and sedimentary signals from the same location. We discuss potential causes of the discrepancy below.

Diagenetic processes resulting in alkenone degradation can be excluded for the reasons described above. Mixing with older sediment by bioturbation may be disregarded for the following reasons: Considering that the sedimentation rate at a site (39.78°N, 70.8°W) near our mooring site was 13 cm/kyr (Tanaka et al., 1991), and that the sediment mixed layer is likely to exceed 14 cm (Tanaka et al., 1991; Anderson et al., 1994), the core-top sediment (0–1 cm) will contain the organic matter produced over several hundred years. However, there is no evidence that SST was markedly colder in this region during the recent history (Keigwin et al., 2003; Sachs, 2007). SST during the Little Ice Age was reported to be only about 1 °C lower than today in the Sargasso Sea (Keigwin, 1996), and hence inclusion of alkenones produced during that time is unlikely to be the cause of the colder $T_{alkenone}$ recorded in the core-top sediment.

The most feasible cause of the discrepancy is lateral supply of resuspended sediment containing a colder $T_{alkenone}$ signal. $T_{alkenone}$ values preserved in sediments "upstream" in the DWBC are cooler because of lower annual average SST (for example, annual average SST at 41°N and 67°W is only 10.8 °C). Hence, entrainment of POM derived from sediments further upslope or upstream of the DWBC would lower $T_{alkenone}$ of sinking POM. It would be necessary to invoke considerably more lateral supply of POM containing a cold $T_{alkenone}$ signal below the 3000 m trap, situated 50 m above the bottom, in order to induce the observed discrepancy between sinking POM and core-top sediment at our site. This may be feasible given the exponential increase in particle concentrations commonly demonstrated by transmissometry gradients near sea floor (John Toole, unpublished data) and the observed low $U^{K'}_{37}$ value of suspended POM collected at 2930 m (0.556 equivalent to 15.3 °C) (Hwang et al., 2009b).

Clearly, there are a number of questions associated with the transfer of alkenones – and more generally POM – from the water column to the underlying sediments. Additional constraints on the provenance and age of alkenones and associated components of sinking and laterally transported particles are needed to resolve these questions. Overall, it is important to consider both vertical and lateral processes in understanding links between surface ocean productivity, water column fluxes, and their manifestations in underlying sediments.

5. Summary

Findings from a study of concentration and flux of C_{37} alkenones, and $U^{K'}_{37}$ values in sinking POM collected at three depths and in the underlying surface sediment on the NW Atlantic margin can be summarized as follows.

- Temporal variations in $T_{alkenone}$ resembled that of the satellite-derived SST at an upstream region in the northeast of the mooring site.
- Although fine-scale variability in $T_{alkenone}$ tracked SST in an upstream region reasonably well, there was significant discrepancy between $T_{alkenone}$ and SST.
- Alkenone flux decreased markedly between 1000 m and 2000 m but by a much lesser degree between 2000 m and 3000 m. $U^{K'}_{37}$ does not appear to be significantly altered during the vertical transit despite a five-fold decrease in alkenone flux.
- Degradation of alkenones was more efficient when alkenone flux was high. Potential temperature bias toward the temperature of high flux period was ameliorated with increasing water depth, implying that temperature biases may vary as a function of the depositional setting (e.g., length of the water column).
- The smaller amplitude of seasonal variation in $T_{alkenone}$ at 2000 m and 3000 m than 1000 m may have been caused by incorporation of suspended POM, potentially including resuspended sediment.
- $T_{alkenone}$ of core-top sediment was lower than flux-weighted $T_{alkenone}$ of sinking POM at 50 m above the seafloor by about 2 °C, which may reflect the additional supply of resuspended sediment carrying alkenones produced in cooler waters to the northeast and transported in the bottom nepheloid layer.

Acknowledgments

We thank F. Batista, L. Costello, A. Dickens, N. Drenzeck, R. François, A. Gagnon, D. Griffith, L. Hmelo, J. Holtvoeth, M. Lardie, W. Martin, D. McCorkle, C. Payne, E. Roosen, J. Saenz, and M. Soon for help with sampling. We thank F. Prahl and two anonymous reviewers for their insightful and constructive suggestions. We acknowledge help from the captains and crews on the R/V *Endeavor* and R/V *Oceanus*. This research was funded by the NSF Ocean Sciences Chemical Oceanography program (OCE-0425677; OCE-0851350) and Ocean and Climate Change Institute of Woods Hole Oceanographic Institution. JH and MK were partly supported by the Korea Research Foundation Grant funded by the Korean Government (2011-0013629).

Appendix A. Supporting information

Supplementary data associated with this article can be found in the online version at http://dx.doi.org/10.1016/j.dsr.2013.10.003.

References

Abramson, L., Lee, C., Liu, Z., Wakeham, S.G., Szlosek, J., 2010. Exchange between suspended and sinking particles in the northwest Mediterranean as inferred from the organic composition of in situ pump and sediment trap samples. Limnol. Oceanogr. 55, 725–739.

Anderson, R.F., Rowe, G.T., Kemp, P.F., Trumbore, S., Biscaye, P.E., 1994. Carbon budget for the mid-slope depocenter of the Middle Atlantic Bight. Deep-Sea Res. II 41, 669–703.

Bacon, M.P., Huh, C.-A., Fleer, A.P., Deuser, W.G., 1985. Seasonality in the flux of natural radionuclides and plutonium in the deep Sargasso Sea. Deep-Sea Res. 32, 273–286.

Benthien, A., Müller, P.J., 2000. Anomalously low alkenone temperatures caused by lateral particle and sediment transport in the Malvinas Current region, western Argentine Basin. Deep-Sea Res. I 47, 2369–2393.

Berelson, W.M., 2002. Particle settling rates increase with depth in the ocean. Deep-Sea Res. II 49, 237–251.

Brassell, S.C., Eglinton, G., Marlowe, I.T., Pflaumann, U., Sarnthein, M., 1986. Molecular stratigraphy: a new tool for climatic assessment. Nature 320, 129–133.

Conte, M.H., Sicre, M.-A., Ruhlemann, C., Weber, J.C., Schulte, S., Schulz-Bull, D., Blanz, T., 2006. Global temperature calibration of the alkenone unsaturation

index ($U^{K'}_{37}$) in surface waters and comparison with surface sediments. Geochem. Geophys. Geosyst. 7, Q02005, http://dx.doi.org/10.1029/2005GC001054.
Conte, M.H., Ralph, N., Ross, E.H., 2001. Seasonal and interannual variability in deep ocean particle fluxes at the Oceanic Flux Program (OFP)/Bermuda Atlantic Time Series (BATS) site in the western Sargasso Sea near Bermuda. Deep-Sea Res. II 48, 1471–1505.
Conte, M.H., Dickey, T.D., Weber, J.C., Johnson, R.J., Knap, A.H., 2003. Transient physical forcing of pulsed export of bioreactive material to the deep Sargasso Sea. Deep-Sea Res. I 50, 1157–1187.
Dennett, M.R., Manganini, S.J., 2006. PCR amplification of preserved ocean flux material. Eos Trans. AGU 87 (36). (Ocean Sci. Meet. Suppl., Abstract OS46D-09).
Goni, M.A., Hartz, D.M., Thunell, R.C., Tappa, E., 2001. Oceanographic considerations for the application of the alkenone-based paleotemperature $U^{K'}_{37}$ index in the Gulf of California. Geochim. Cosmochim. Acta 65, 545–557.
Harada, N., Handa, N., Harada, K., Matsuoka, H., 2001. Alkenones and particulate fluxes in sediment traps from the central equatorial Pacific. Deep-Sea Res. I 48, 891–907.
Herbert, T.D., 2003. Alkenone paleotemperature determinations. In: Elderfield, H. (Ed.), The Oceans and Marine Geochemistry. Elsevier-Pergamon, Oxford, pp. 391–432.
Honjo, S., Doherty, K.W., 1988. Large aperture time-series sediment traps; design objectives, construction and application. Deep-Sea Res. 35, 133–149.
Hwang, J., Manganini, S.J., Montlucon, D.B., Eglinton, T.I., 2009a. Dynamics of particle export on the Northwest Atlantic margin. Deep-Sea Res. I 56, 1792–1803.
Hwang, J., Montlucon, D., Eglinton, T.I., 2009b. Molecular and isotopic constraints on the sources of suspended particulate organic carbon on the northwestern Atlantic margin. Deep-Sea Res. I 56, 1284–1297.
Joyce, T.M., Dunworth-Baker, J., Pickart, R.S., Torres, D., Waterman, S., 2005. On the Deep Western Boundary Current south of Cape Cod. Deep-Sea Res. II 52, 615–625.
Keigwin, L., 1996. The little ice age and medieval warm period in the Sargasso Sea. Science 274, 1503–1508.
Keigwin, L.D., Sachs, J.P., Rosenthal, Y., 2003. A 1600-year history of the Labrador Current off Nova Scotia. Clim. Dyn. 21, 53–62.
Knappertsbusch, M., Brummer, G.-J.A., 1995. A sediment trap investigation of sinking coccolithophorids in the North Atlantic. Deep-Sea Res. 42, 1083–1109.
Kusch, S., Eglinton, T.I., Mix, A.C., Mollenhauer, G., 2010. Timescales of lateral sediment transport in the Panama Basin as revealed by radiocarbon ages of alkenones, total organic carbon and foraminifera. Earth Planet. Sci. Lett. 290, 340–350.
Mollenhauer, G., McManus, J.F., Benthien, A., Müller, P.J., Eglinton, T.I., 2006. Rapid lateral particle transport in the Argentine Basin: molecular ^{14}C and $^{230}Th_{xs}$ evidence. Deep-Sea Res. I 53, 1224–1243.
Müller, P.J., Fischer, G., 2001. A 4-year sediment trap record of alkenones from the filamentous upwelling region off Cape Blanc, NW Africa and a comparison with distributions in underlying sediments. Deep-Sea Res. I 48, 1877–1903.
Ohkouchi, N., Eglinton, T.I., Keigwin, L.D., Hayes, J.M., 2002. Spatial and temporal offsets between proxy records in a sediment drift. Science 298, 1224–1227.
Prahl, F.G., Wakeham, S.G., 1987. Calibration of unsaturation patterns in long-chain ketone compositions for palaeotemperature assessment. Nature 330, 367–369.
Prahl, F.G., Collier, R., Dymond, J., Lyle, M., Sparrow, M.A., 1993. A biomarker perspective on prymnesiophyte productivity in the northeast Pacific Ocean. Deep-Sea Res. I 40, 2061–2076.
Rontani, J.-F., Volkman, J.K., Prahl, F.G., Wakeham, S.G., 2013. Biotic and abiotic degradation of alkenones and implications for $U^{K'}_{37}$ paleoproxy applications: a review. Org. Geochem. 59, 95–113.
Rosell-Melé, A., Prahl, F.G., 2013. Seasonality of U^{K}_{37} temperature estimates as inferred from sediment trap data. Q. Sci. Rev. 72, 128–136.
Ruhlemann, C., Butzin, M., 2006. Alkenone temperature anomalies in the Brazil-Malvinas Confluence area caused by lateral advection of suspended particulate material. Geochem. Geophys. Geosyst. 31, Q10015 (10010.11029/12006GC001251).
Sachs, J.P., 2007. Cooling of Northwest Atlantic slope waters during the Holocene. Geophys. Res. Lett. 34, L03609 (03610.01029/02006GL028495).
Sachs, J.P., Schneider, R.R., Eglinton, T.I., Freeman, K.H., Ganssen, G., McManus, J.F., Oppo, D.W., 2000. Alkenones as paleoceanographic proxies. Geochem. Geophy. Geosyst. 1 (000059), 2000GC.
Seki, O., Nakatsuka, T., Kawamura, K., Saitoh, S.-I., Wakatsuchi, M., 2007. Time-series sediment trap record of alkenones from the western Sea of Okhotsk. Mar. Chem. 104, 253–265.
Sheridan, C.C., Lee, C., Wakeham, S.G., Bishop, J.K.B., 2002. Suspended particle organic composition and cycling in surface and midwaters of the equatorial Pacific Ocean. Deep-Sea Res. I 49, 1983–2008.
Shutler, J.D., Land, P.E., Brown, C.W., Findlay, H.S., Donlon, C.J., Medland, M., Snooke, R., Blackford, J.C., 2012. Coccolithophore surface distributions in the North Atlantic and their modulation of the air-sea flux of CO_2 from 10 years of satellite Earth observation data. Biogeosci. Discuss. 9, 5823–5848.
Siegel, D.A., Deuser, W.G., 1997. Trajectories of sinking particles in the Sargasso Sea: modeling of statistical funnels above deep-ocean sediment traps. Deep-Sea Res. I 44, 1519–1541.
Siegel, D.A., Fields, E., Buesseler, K.O., 2008. A bottom-up view of the biological pump: modeling source funnels above ocean sediment traps. Deep-Sea Res. I 55, 108–127.
Tanaka, N., Turekian, K.K., Rye, D.M., 1991. The radiocarbon, $\delta^{13}C$, ^{210}Pb, and ^{137}Cs record in box cores from the continental margin of the Middle Atlantic Bight. Am. J. Sci. 291, 90–105.
Toole, J.M., Curry, R.G., Joyce, T.M., McCarthy, M., Pena-Molino, B., 2011. Transport of the North Atlantic Deep Western Boundary Current about 39°N, 70°W: 2004–2008. Deep-Sea Res. II 58, 1768–1780.
Yoder, J.A., O'Reilly, J.E., Barnarda, A.H., Moore, T.S., Ruhsam, C.M., 2001. Variability in coastal zone color scanner (CZCS) Chlorophyll imagery of ocean margin waters off the US East Coast. Cont. Shelf Res. 21, 1191–1218.